



Influence of torsional irregularity on tri-directional floor response spectra used in industrial buildings

Meenakshi V. Landge¹ · Ramakant K. Ingle¹

Received: 7 June 2021 / Accepted: 31 August 2021 / Published online: 12 October 2021
© Springer Nature Switzerland AG 2021

Abstract

The need for industrial buildings has increased multifold, with a wide range in the irregular distribution of floor mass and stiffness. The uneven distribution of floor mass causes mass eccentricity in the floor, inducing torsion in the building. The aim of the present study is to highlight the influence of torsional irregularity due to mass eccentricity on the multi-directional floor response spectra. IS 1893 (Part 4): 2015 suggested time-history analysis of the design basis earthquake to develop floor response spectra, adopting linear analysis technique. Eleven sets of real orthogonal records were chosen to perform time-history analysis to obtain a mean response. The present study observed that the building's with regular geometry and without stiffness variation in it, a slight mass eccentricity significantly increases floor response spectra. Moreover, actual industrial buildings have significant variations in mass, stiffness, and strength, resulting in further intensifying floor response spectra. Thus, the structural designer needs to use tri-directional floor response spectra for precise and protective non-structural component support design for appropriate response. IS 1893 (Part 1): 2016 suggests reduced stiffness for beam and column for earthquake analysis. Floor response spectra with reduced stiffness were also studied here, and the response was compared with non-linear analysis. Non-structural components lateral design forces as per floor response spectra approach and Indian Standard provisions are also included in the study.

Keywords Industrial buildings · Seismic design · Non-structural component · Time-history analysis · Floor response spectra · Torsional irregularity

Introduction

In recent years, the demand for industrial structures has surged, supporting a wide range of equipment and operations, especially vertically. Buildings have basic structural elements (beam, column, and slab) as the primary structural system to support the secondary system. The secondary systems, also referred to as non-structural components (NSCs), include mechanical (boilers, hoppers, storage tanks, piping systems, fire prevention systems, water supply units, and heating ducts) and electrical (electric motors, interior fittings, power supply units, HVAC units, and elevators) components, etc. The loss of NSCs after the earthquake is something greater than structural damage [1]. These losses

are divided into direct property damage and indirect economic losses [1].

The preliminary study on the NSC response started with caution and safety of the nuclear power plant's critical components [2]. After this preliminary study, the US Nuclear Regulatory Guide [3] was established. Many researchers [4–14] stated in their studies that floor response spectra (FRS) is required to get the acceleration demand on NSCs. Medina et al. [15] noted that the placement of NSCs on primary structures influenced the shape and magnitude of FRS. Also, the yielding of the main structure has a complex impact on the NSC reaction. Further, [16–18] perceived remarkable differences in the acceleration demand on NSC are due to ground motion characteristics, higher mode effects, and different building irregularities.

FRS could be established through a direct spectra-to-spectra approach or a time-history analysis (THA) approach [19]. In the study by Duff [20], a single selection of earthquake excitation in three directions was used to monitor FRS, and the author discovered that the FRS obtained was

✉ Meenakshi V. Landge
mjdvnit2015@gmail.com

¹ Department of Applied Mechanics, Visvesvaraya National Institute of Technology, South Ambazari Road, Nagpur, Maharashtra 440010, India

not accurate. As a result, FRS can necessitate a more significant number of sets of earthquake excitation in three directions to get a reliable probabilistic definition.

Singh [11, 21] introduced the concept of random vibration for a direct approach and researchers [2, 22, 23] developed a study on direct spectra-to-spectra techniques to lighten the limitations of THA approaches. The FRS methodically communicated with the modal analysis parameters (frequencies, mode shapes, and modal participation factors) and ground motion spectra of the primary structure in the direct method. Since the 1970s, many direct spectra-to-spectra methods for obtaining FRS have been available. Still, they have not been widely employed in the nuclear sector because it is uncertain how conservative or unconservative the FRS is. The FRS results should be conservative, but not excessively so; otherwise, the cost of seismic qualification and components would vary dramatically.

The various studies [11, 13, 24–29] on THA converge to smooth mean and median FRS. And [14, 30–35] considered the smooth mean, median FRS generated by THA as exact FRS and used it as a baseline to verify the direct method's accuracy. Further, the researchers [29, 32, 33] generated FRS based on a decoupling analysis, revealing that the equipment's interaction with the supporting structure is minimal.

As per IS1893 (Part 4): 2015 [36], for the development of FRS, THA should be performed for design basis earthquake (DBE), adopting a linear analysis technique. Also, it stated that if the ratio of the mass of flexible mounted equipment to the sum of the mass of the primary structural system and the mass of rigidly mounted equipment is less than 0.25, then no interaction between the primary structures and the equipment should be considered. In such a case, flexible mounted equipment's mass should be considered lumped at appropriate locations. The aim of the present study is to highlight the influence of torsional irregularity due to mass eccentricity on the Tri-directional FRS used in industrial buildings. For comparative analysis, G + 2 storey, regular building, and torsional irregular building with irregular mass distribution are considered, and their elastic FRS response studied. IS 1893 (Part 1): 2016 [37] suggests reduced stiffness for beam and column for earthquake analysis. Therefore, elastic FRS with reduced stiffness was also studied at considered NSC locations with appropriate lump mass and response compared with non-linear analysis. For THA, actual ground motion records were obtained using the PEER NGA-West 2 [38] database. The study was carried out using the SAP-2000 [39] computer software.

Limitations of the study

The study's outcomes are limited to low-rise reinforced concrete special moment-resisting bare frame structures

that were analysed assuming most of the industrial buildings are having few infill walls and are designed according to [36, 37, 40–42] for a specific input. In the current analytical work, the influence of soil-structure interaction was also neglected. The building on soft strata may change the structural parameters. The paper does not include any experimental validation.

Details of buildings considered for study

The behaviour of a building during an earthquake depends on several factors. The present study included a G + 2 storey, three bays, reinforced concrete (RC) low-rise three-dimensional building. Buildings are analysed with a special moment-resisting frame (SMRF). Geometric details of buildings with beam and column positions are shown in Fig. 1. A storey height of 3 m and a bay width of 4 m were taken for the buildings. The comparative analytical study considered a regular building (RB) and another RC building with torsional irregularity (TIRB). The TIRB has the same geometry and stiffness as the RB but an unequal distribution of floor mass (Fig. 1a and b). The unequal distribution of floor mass has been considered by varying brick wall load and live load on the slab, as shown in Fig. 1-b. This floor mass variation is constant on all three floors. The brick wall is 230 mm thick, and the floor slab is 150 mm thick with floor finish load and live load of 1 kN/m² and 5 kN/m², respectively, considered as per Indian standard IS 875: Part 1 and Part 2 [43, 44].

Each floor has mass eccentricity in the X and Y directions because of the uneven distribution of floor mass. Table 1 shows the positions of the centre of mass (X-CM, Y-CM), the centre of rigidity (X-CR, Y-CR), and eccentricity (e_x , e_y) in the analysed buildings. The varying horizontal displacement at the extreme end of the identical floor is induced by this eccentricity. As per IS 1893 (Part 1): 2016 [37], a building is torsionally irregular if the maximum horizontal displacement at one end of the floor is larger than 1.5 times the minimum displacement at the other end of the same level in the same direction. Table 2 illustrates the horizontal displacement in the X direction at the two ends of the identical floor for both buildings. The RB building model has the same horizontal displacement at the floor ends, as shown in Table 2. However, the maximum displacement (at grid 1-D) of the same floor in the same direction in the TIRB building model is larger than 1.5 times the minimum displacement (at grid 4-D) of the same floor in the same direction for all three stories. As a result, the TIRB building was classified as a torsionally irregular structure, satisfying the torsional irregularity clause of IS 1893 (Part 1): 2016 [37].

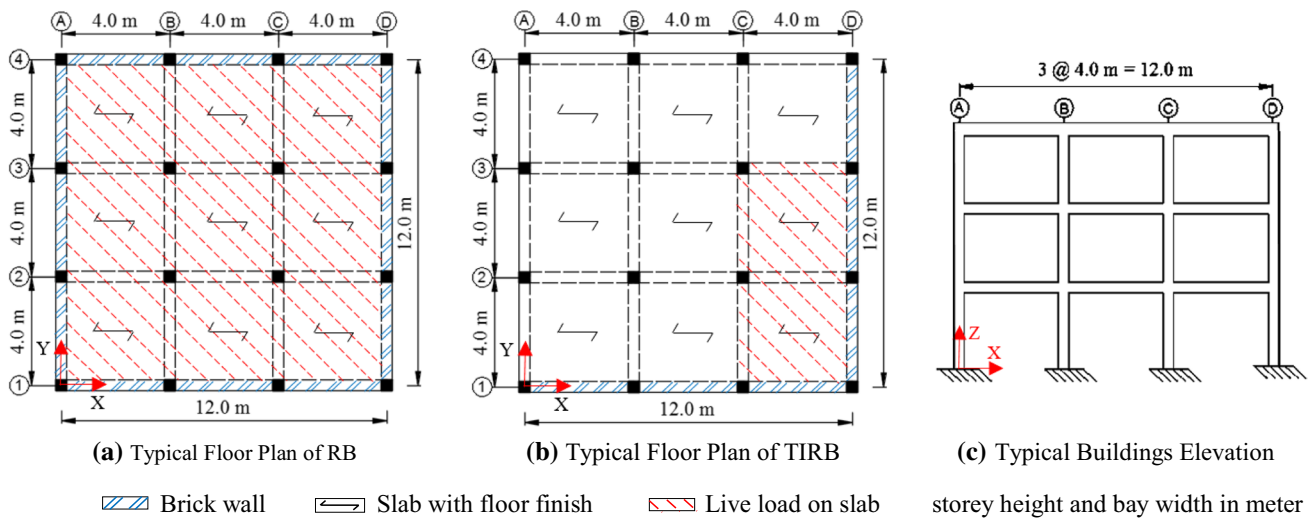


Fig. 1 G+2 Storey RC Buildings

Table 1 Mass eccentricity in building (m)

Building Model	RB						
	Storey Number	X-CM	Y-CM	X-CR	Y-CR	ex	ey
3	6	6	6	6	0	0	
2	6	6	6	6	0	0	
1	6	6	6	6	0	0	
Building Model	TIRB						
	3	6.90	5.22	6.00	6.00	0.90	-0.78
	2	6.86	5.26	6.00	6.00	0.86	-0.74
1	6.86	5.26	6.00	6.00	0.86	-0.74	

Table 2 Horizontal X-direction displacement (mm)

Building Model	RB		TIRB	
	Storey Number	Grid 1-D	Grid 4-D	Grid 1-D
3	25	25	23	14
2	19	19	17	10
1	9	9	8	5

The building’s location is considered in zone V [37] (i.e. the highest seismic zone in India) and is located on medium soil. M30 grade concrete was used to model the RC beams and columns. Floor diaphragms were considered to be rigid in the analysis. The building is designed as per codal requirements, and the designed sizes are adopted. It is also ensured that the total column design strength is 1.4 times that of the beam design strength at every beam-column joint. To prevent further strength and stiffness irregularities in the building, the beam size (230 mm × 400 mm) and column size (350 mm × 350 mm)

in the RB and TIRB buildings have been kept constant in all three stories.

Dynamic properties of buildings

The dynamic analysis was performed for RB and TIRB buildings, and the linear mode shapes and corresponding periods for the first five modes are shown in Fig. 2 and Table 3. The modal participation mass ratio for the RB and TIRB building models in each mode is illustrated in Table 4. It shows that mass participation in the third mode (torsional mode) in the X and Y directions is zero in the RB model. In contrast, in the TIRB model, mass participation in the third mode in the X and Y directions is 8% and 11%, respectively, indicating torsional behaviour. In this study, a total of twelve modes were considered. The Indian standard [37] specifies that the number of modes in the analysis is to be considered until the total mass participation exceeds 90%. Table 5 illustrates the cumulative modal mass participation. The cumulative mass participation exceeds 90% in the fifth mode, which is observed in Table 5.

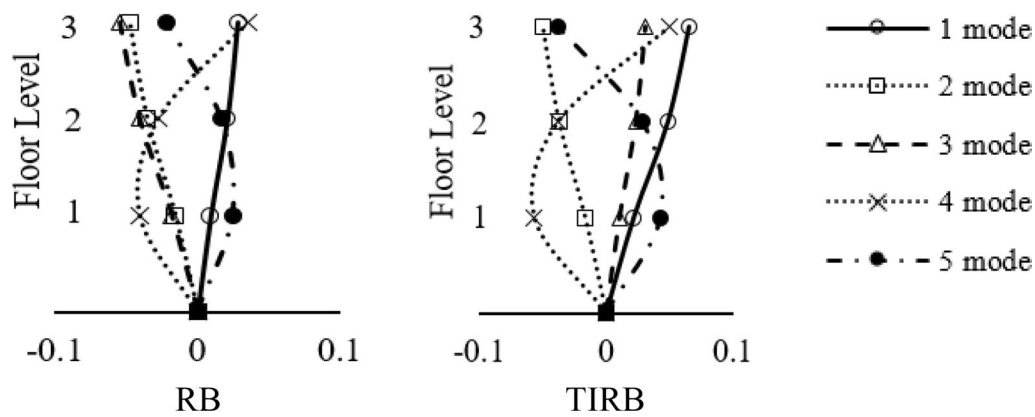


Fig. 2 Linear mode shapes for considered building models

Table 3 Modal Periods (sec)

Building Model	Mode 1	Mode 2	Mode 3	Mode 4	Mode 5
RB	0.61	0.61	0.57	0.19	0.19
TIRB	0.54	0.51	0.44	0.17	0.16

Floor response spectra (FRS)

An acceleration time-history on each building floor obtained from the base excitation must be used to design the NSCs supports attached to the floor. IS 1893 (Part 4): 2015 [36] says that FRS is necessary for NSC analysis and design in critical conditions. It also said that when the ratio of the mass of flexible mounted equipment to the sum of the mass of the primary structural system and the mass of rigidly mounted equipment is less than 0.25, then no interaction between the primary structures and the equipment should be considered, which is called decoupled analysis. In such a case, flexible mounted equipment’s

mass should be considered lumped at appropriate locations. On the other hand, when the ratio is greater than 0.25, the interaction between the equipment support and the primary structure should be considered by suitable modelling of the support system, known as coupled analysis. Many researchers [4, 12, 13, 29, 45, 46] in their studies mentioned that FRS is a decoupled analytic method in which the primary and secondary systems are analysed separately. That means the primary structure is subjected to a dynamic study first, with the secondary system’s effects overlooked.

Figure 3 illustrates that the appropriate ground motion histories are used as input for the primary structure analysis. Then, the responses of the primary structure at the nth floor, i.e. the floor’s acceleration history, are fed into an SDOF system to generate FRS. As a result, FRS estimated the maximum response for the NSC design. Figure 3 also shows that the floor’s acceleration time-history is not the same as the ground’s acceleration time-history. Seismic excitation in both orthogonal horizontal and vertical directions is commonly used in seismic design (Fig. 3). The FRS is evaluated

Table 4 Modal Participating Mass Ratio in Each Mode

Building Model	Mode No	1	2	3	4	5	6
RB	UX	0.22	0.64	0.00	0.08	0.03	0.00
	UY	0.64	0.22	0.00	0.03	0.08	0.00
TIRB	UX	0.29	0.49	0.08	0.04	0.06	0.01
	UY	0.38	0.37	0.11	0.05	0.05	0.01

Table 5 Cumulative Modal Participating Mass Ratios

Building Model	Mode No	1	2	3	4	5	6
RB	UX	0.22	0.86	0.86	0.94	1.00	1.00
	UY	0.64	0.86	0.86	0.89	0.97	0.97
TIRB	UX	0.29	0.78	0.86	0.90	1.00	1.00
	UY	0.38	0.75	0.86	0.91	0.96	0.97

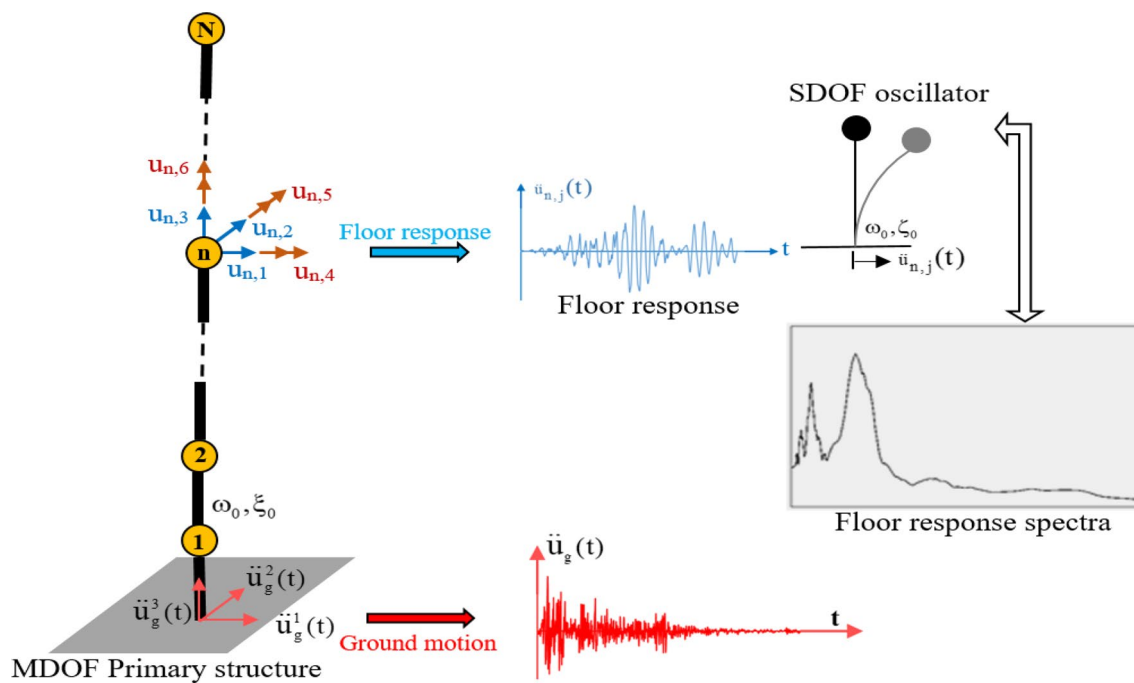


Fig. 3 Generation of FRS

on the required floor of the building using standard dynamic theory. To study the influence of torsional irregularity on the tri-directional FRS input time-history as per subsequent section, has been considered.

Input time-history

According to [47–50], simulated or artificial accelerograms generate a scattered and unrealistic response. As a corollary, [51–54] encourages the use of real ground motion data. Thus, an actual ground motion database has been obtained using the PEER NGA-West 2 [38]. Time-history analysis for DBE adopting linear analysis technique is required for the development of FRS [36]. A total of 11 sets of real orthogonal records were considered to obtain mean responses to perform tri-directional time-history analysis [55–57]. Table 6 shows the key properties of the selected ground motions. The selected records have moment magnitudes ranging from 6 to 7. The nearest horizontal distance to the rupture plane’s surface projection (Joyner Boore distance ‘Rjb’ in kilometres) varied from 10 to 30 km. In addition, Table 6 shows the average shear wave velocity of the top 30 (Vs30) metres of soil.

The IS 1893 (Part 1): 2016 [37] DBE zone V target spectra, 11-ground motion individual response spectra, and its mean spectra are represented in Fig. 4. To minimize the record-to-record spectral divergence in the selection of ground motions, an add-on condition of $\pm 50\%$ limit to the

target spectra [47, 58, 59] was utilized. In addition, as per the amplitude-scaling clause [19], the mean spectra should not be underneath 90% of the target spectra in the indicated period range. This period range’s upper limit is twice the most significant first mode period. In addition, the period range covering at least the number of modes required to attain 90% mass participation is the smaller limit. Figure 4 shows the mean spectra that satisfy the criteria described above.

In this investigation, the computer software SAP-2000 [39] was used to numerically solve the dynamic equation of motion using the step-by-step linear acceleration approach. As discussed earlier section, the beam and column moment-resisting frames with rigid floor diaphragms are used to model the lateral force-resisting systems. The RB and TIRB building models were subjected to ground motion data. The FRS with 5% damping was produced, and the results are presented in the discussion below.

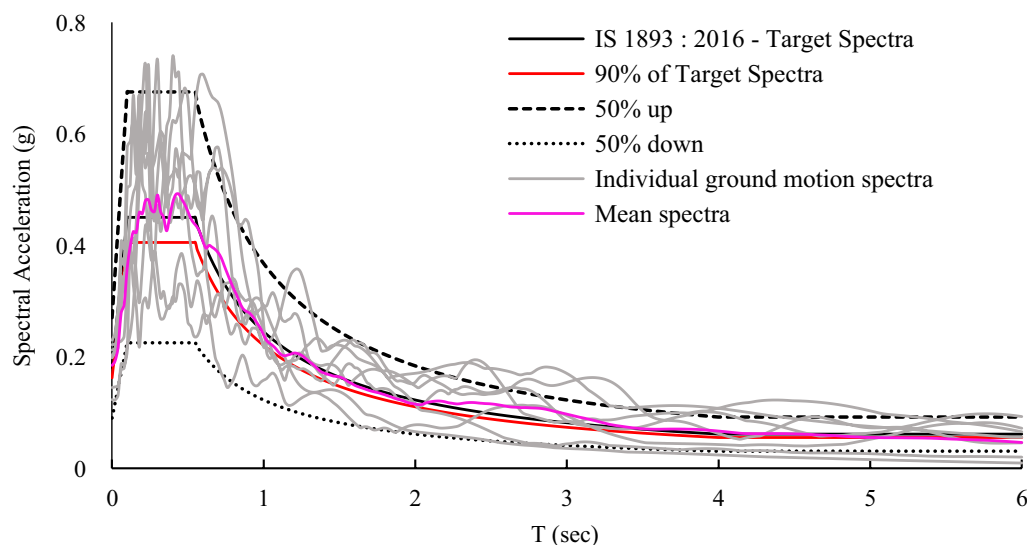
Results and observations

Elastic FRS of RB and TIRB buildings

Linear time-history assessments under 11 earthquake records (as revealed in previous section) in two horizontal (X and Y) and one vertical (Z) directions were conducted individually. Elastic FRS for each ground motion at the different nodes of the gridlines of the entire three floors was

Table 6 Selected ground motions details

Earthquake	Record Sequence Number	Magnitude	Station	Year	V_{s30} (m/sec)	R_{jb} (km)
Imperial Valley-06	169	6.53	Delta	1979	242.05	22.03
Superstition Hills-02	728	6.54	Westmorland Fire Sta	1987	193.67	13.03
Spitak_Armenia	730	6.77	Gukasian	1988	343.53	23.99
Loma Prieta	777	6.93	Hollister City Hall	1989	198.33	27.33
Northridge-01	960	6.69	Canyon Country—W Lost Cany	1994	325.6	11.39
Kobe Japan	1116	6.9	Shin-Osaka	1995	256	19.14
Chuetsu-oki Japan	4883	6.8	Niigata Nishi Kaba District	2007	254.68	27.83
Iwate Japan	5774	6.9	Nakashinden Town	2008	276.3	29.37
Darfield New Zealand	6953	7.0	Pages Road Pumping	2010	206	24.55
Darfield New Zealand	6969	7.0	Styx Mill Transfer	2010	247.5	20.86
Christchurch New Zealand	8134	6.2	Styx Mill Transfer	2011	247.5	11.24

**Fig. 4** IS 1893 DBE Target spectra, 11-ground motion record sets individual response spectra and its mean spectra

obtained. In this section, the final FRS result is the mean FRS obtained from these 11 linear time-history analyses. It is essential to compute the spectrum ordinates at the fundamental natural period of the primary structure or at a sufficiently close period, which results in valid response spectra [3]. When the FRS is plotted over a wide number of periods, maximum spectrum peaks should emerge at the fundamental natural period of the supporting structure [60]. For the FRS results with 5% damping, the vertical axis indicates the mean spectral acceleration ‘ S_a ’ in g units, and the horizontal axis is used to indicate the period ‘ T ’ in seconds.

Figures 5a and b show the first to third floor’s acceleration FRS for RB in X and Y orthogonal directions when subjected to seismic excitation in X and Y, respectively. The FRS examinations revealed a gradual increase in

response from the lower to the highest floors [15, 61, 62]. It is apparent that the spectrum shows maximum peaks at the first mode period of RB (shown by the black dotted line), i.e. $T = 0.61$ s [60]. Because of modal interaction, energy can be transferred from the fundamental mode to higher modes [63], resulting in a peak in the spectrum during the 4th mode period also (i.e. $T = 0.19$ s, as indicated by the red dotted line).

According to the study, FRS spectral accelerations were also enhanced compared to ground spectral accelerations (i.e. mean spectra as per previous section). Kumar et al. [57], Maddaloni [64], and Petrone et al. [65] found similar results in their studies. In addition, [24, 66, 67] stated that the FRS at lower floors tends to follow the input ground

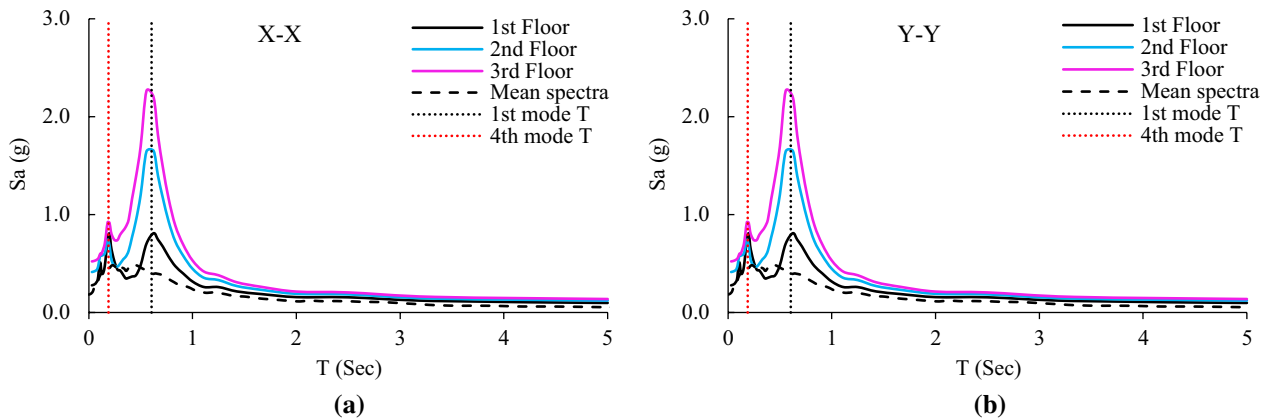


Fig. 5 FRS results for RB

motion spectra and its properties influence the NSC support design at lower floors.

The node-to-node response on each grid in the X, Y, and Z directions has been examined in the RB model for earthquake excitation in the X, Y, and Z directions. It is noticed that the RB model only shows the response when the earthquake excitation and response directions are the same. If the earthquake excitation direction is X and the response direction is Y and vice versa, no response quantities have been obtained. The spectral acceleration in the Z direction using earthquake excitation in the Z direction as input was determined to be very low. Hence, the data is not shown. The X and Y direction FRS for X and Y earthquake excitation direction is found to be identical in the RB model, which can be observed in Fig. 5.

In the TIRB model, node-to-node response on each grid was evaluated in the X, Y, and Z directions following earthquake excitation in the X, Y, and Z directions, respectively. It has been observed that nodes on the same grid have the same response when earthquake excitation is parallel to the grid, while nodes on other parallel grids have different responses. (i.e. Grid-1 nodes (A-1, B-1, C-1, and D-1) indicate the same response in the X direction when the earthquake excitation direction is X, while Grid-2, Grid-3, and Grid-4 responses will differ from grid-1 for the X-seismic excitation direction). In addition, when the earthquake excitation direction is X, nodes on Grid-1 (A-1, B-1, C-1, and D-1) indicate different responses in the Y direction. It will also be applicable if the earthquake excitation and response directions are altered in the manner described above. Based on this, Fig. 6a–f indicates the FRS results of TIRB for earthquake excitation directions X and Y. The results are not presented because the spectral acceleration in the Z direction is found to be very low with earthquake excitation in the Z direction as input.

The FRS increases in response from lower to upper levels in the TIRB model as well. For comparative study, only

upper floor findings, i.e. 3rd floor results, are given in Fig. 6. It shows a FRS with the highest peak near the 1st mode period of the TIRB model (i.e. $T = 0.54$ s, as indicated by the dotted line). Like the RB model, in the TIRB model, a peak in the spectrum during the 4th mode period has been observed (i.e. $T = 0.17$ s, as indicated by the red dotted line). Also, the 3rd mode period shows the maximum spectral peak in Grid A (Fig. 6b) and Grid 1 (Fig. 6d).

The FRS maximum spectral peaks in the Y direction response are nearly 60% than in the X direction response, as shown in Figs. 6a and b. The same observation is observed in Figs. 6c and d, where the earthquake excitation input changed to the Y direction. Thus, when the earthquake and response directions are the same, the peak spectral acceleration is higher. Furthermore, the peak spectral acceleration is even higher in the Y direction of earthquake excitation. In addition, Figs. 6e and f exhibit the FRS for X and Y direction earthquake excitation input and Z direction response, respectively, demonstrating that a vertical direction spectral peak exists, but they are minor.

Amplification in floor response in buildings with short periods, i.e. TIRB, is higher than RB. Even though the building’s geometry is regular and there is no stiffness variation in the orthogonal direction, a tiny mass eccentricity can significantly alter the FRS response.

Influence of variation in building stiffness on elastic FRS

For structural analysis of RC buildings, IS 1893 (Part 1): 2016 [37] specifies that the moment of inertia of beams and columns shall be considered as 35% of I_{gross} and 70% of I_{gross} , respectively. The idea of using the moment of inertia factor (MIF) for structural analysis is introduced for the first time in IS 1893 (Part 1): 2016 [37]. Cracks will occur in the concrete’s tension zone due to varying loads applied to the RC members. Therefore, the moment of inertia will

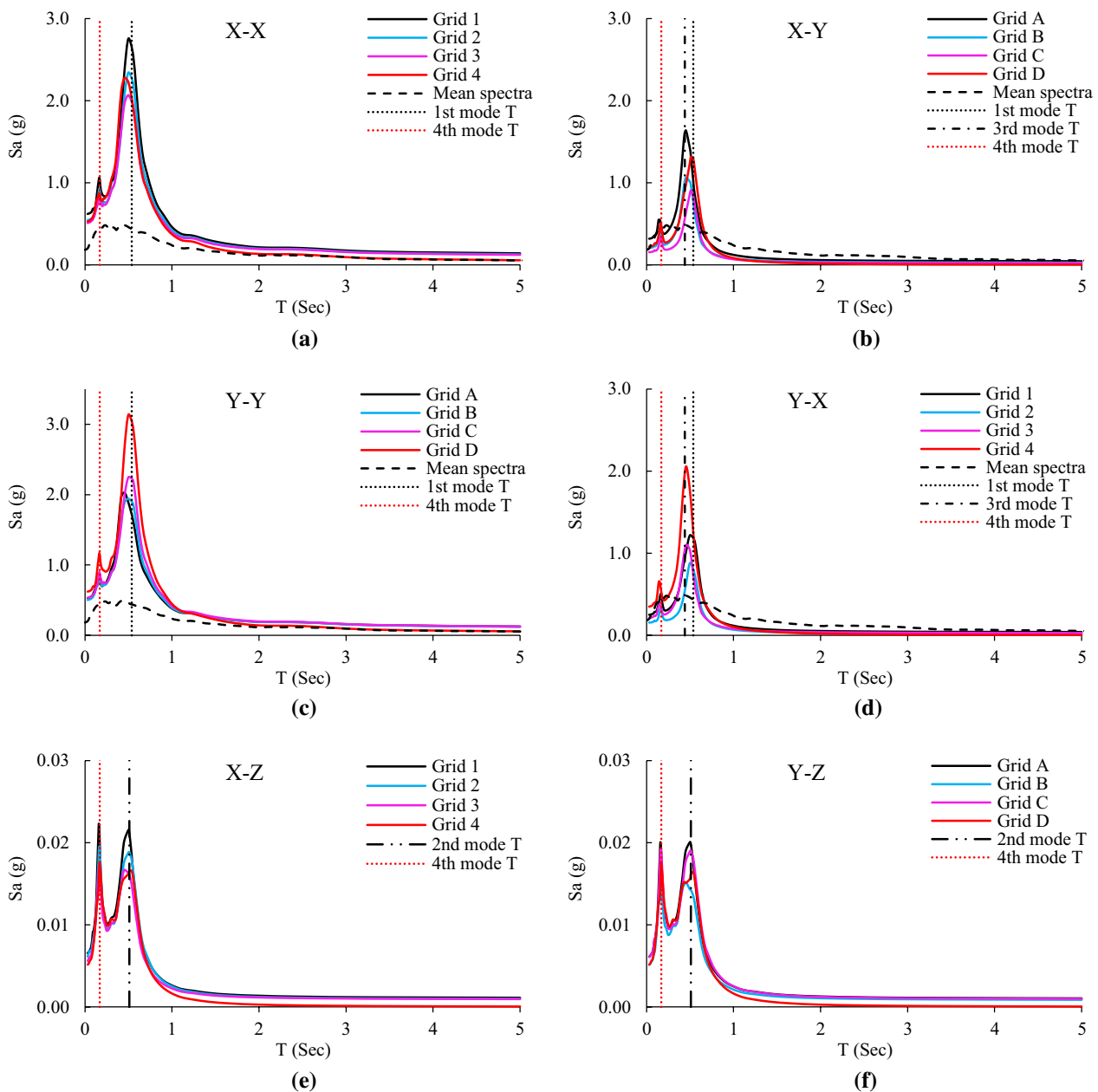


Fig. 6 FRS results for TIRB

be less than the gross moment of inertia of RC members. Thus, the moment of inertia factor (MIF) is used in the code to account for the reduced moment of inertia. In addition, the columns experience more axial compression than the beams; the number of cracks in the columns is lower than the number of cracks in the beams. As a result, the MIF of the column is higher than that of the beam.

As a basis, the comparative analytical investigation included another G + 2-storey TIRB building with MIF. The building model is designated as TIRB-MIF, and its geometry and floor mass distribution are identical to those of the

TIRB building model. As discussed in the introduction, the mass of flexible mounted equipment should be considered a lumped mass at appropriate locations. Therefore, the lumped mass of NSC at P and Q locations on the 3rd floor of the TIRB and TIRB-MIF building models has been considered (as shown in Fig. 7).

The dynamic properties of the TIRB-MIF building model are shown in Table 7. The building's total stiffness is reduced when the moment of inertia of beams and columns is reduced. As a result of the reduced stiffness, the building became comparatively flexible. So the fundamental natural

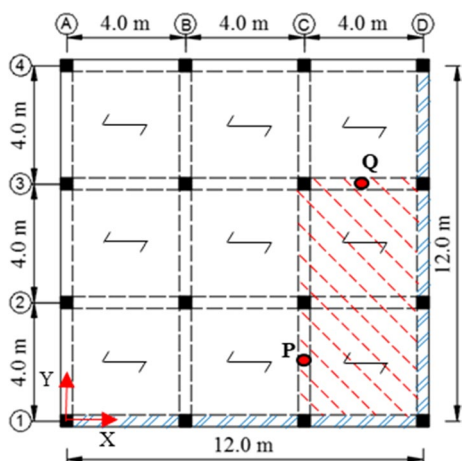


Fig. 7 NSC locations at 3rd Floor of TIRB and TIRB-MIF

period of TIRB-MIF is larger than the TIRB natural period (Table 3 and 7). The cumulative modal participating mass ratio exceeds 90% at the fifth mode, which can be observed in Table 7.

In this part, elastic FRS for X and Y direction excitation was calculated for 11 earthquake data at the P and Q locations. Figure 8 shows the mean FRS response in the X and Y direction for 5% damping. The response of NSC locations at P and Q attached to the TIRB building model is shown with a continuous line, and NSC locations at P and Q attached to the TIRB-MIF building model is shown with a dotted line. As discussed above section, when the earthquake excitation input and FRS response directions are the same, the peak spectral acceleration is higher. The same observation was observed for NSC locations at P and Q, shown in Fig. 8a–d.

The TIRB-MIF building’s total stiffness is reduced when the moment of inertia of beams and columns is diminished. As a result of the reduced stiffness, the structure became comparatively more flexible than the TIRB, attracting fewer seismic forces. The seismic force values are proportional to the building’s spectral acceleration, i.e. the lower the seismic force, the lower the spectral acceleration. As a result, even though the mass values in the TIRB and TIRB-MIF building models are constant, the floor response is reduced by having a lower stiffness.

Elastic and inelastic FRS comparison

To incorporate non-linearity into the building, a lumped plastic hinge model as per ASCE 41–17 [68] has been used to simulate the non-linear behaviour of members. In the non-linear performance assessment of reinforced concrete building models, the non-linear behaviour of beams and columns has been typically represented by concentrated plastic hinges at both ends of the members. In the case of beam members, M3 hinges (i.e. uncoupled moment hinges about the major axis) and for column members, P-M2-M3 hinges (i.e. coupled axial force and biaxial bending moment hinges) have been assigned. In addition, the Takeda Hysteresis model [69] has been used to pretend the degradation of the RC element in the non-linear analysis. This simple hysteric model does not require additional parameters and is also appropriate for reinforced concrete. The non-linear time-history under 11 earthquake records (as revealed in previous section) in two horizontal (X and Y) directions were conducted for the TIRB building with a lumped mass on the 3rd floor (Fig. 7). Elastic and inelastic FRS results of NSC at P location are shown in Fig. 9. It has been noted that inelastic FRS (dash lines) represents a reduction in floor spectral accelerations compared to elastic FRS [24, 70, 71]. But the peak spectral acceleration of inelastic FRS is close to the elastic FRS with MIF building models.

NSC lateral design forces

IS 16700: 2017 [41] codal provisions give the lateral design force formulation for acceleration-sensitive NSC. Therefore, the comparison of NSC design forces as per the FRS approach, and Indian standard Codal provision (at the P location) has been done and is shown in Table 8. The weight of the NSC at the P location has been taken as 20 kN. From Table 8, it can be observed that the NSC is subjected to varying design forces as per the input-response direction in the FRS approach, whereas the Indian standard codal provision gives a single design force. The design force as per IS 16700: 2017 [41] was found to be conservative.

Table 7 Dynamic Properties of TIRB-MIF Model

Mode No		1	2	3	4	5
Period (sec)		0.76	0.72	0.60	0.22	0.21
Modal Participating Mass Ratios	UX	0.30	0.48	0.06	0.04	0.07
	UY	0.40	0.36	0.08	0.06	0.05
Cumulative Modal Participating Mass Ratios	UX	0.30	0.78	0.84	0.88	0.95
	UY	0.40	0.76	0.84	0.90	0.95

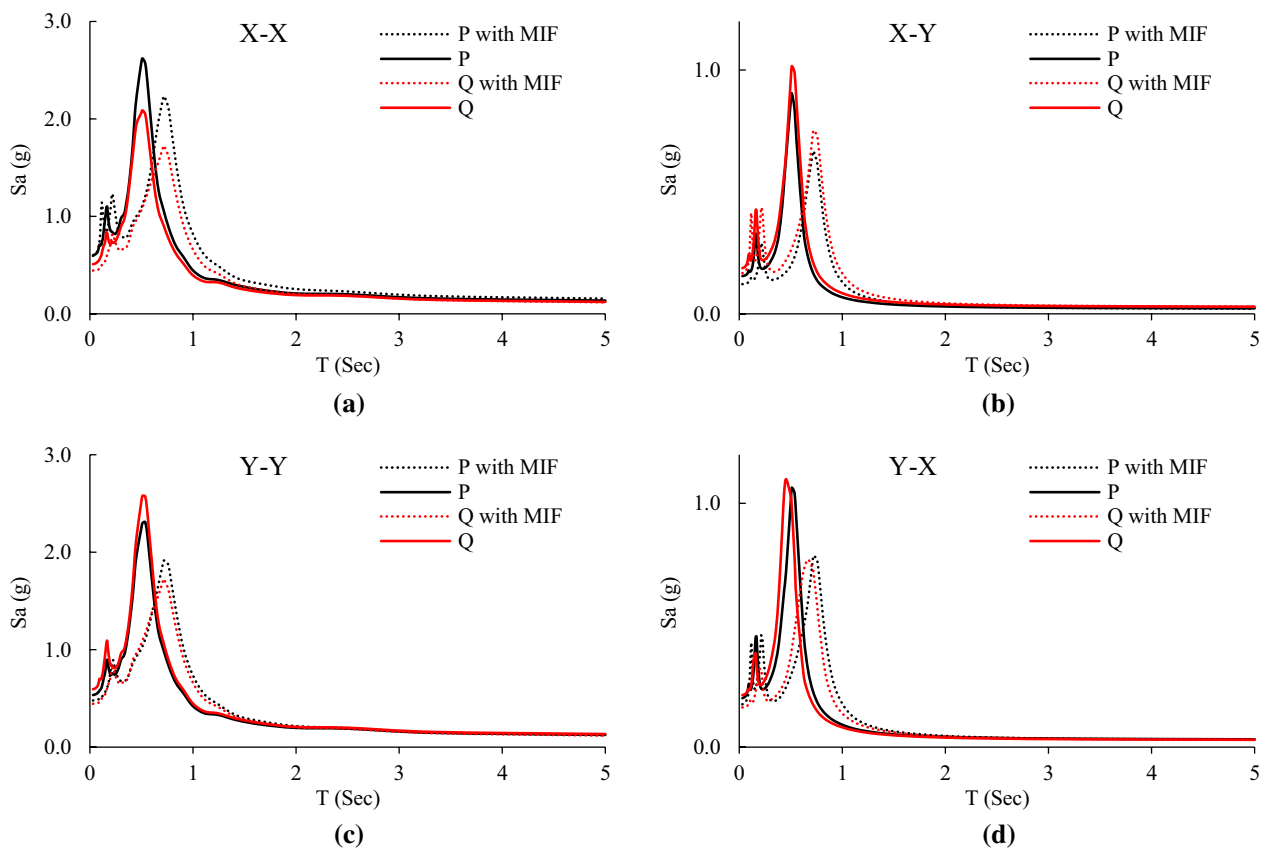


Fig. 8 FRS results at NSC locations P and Q

Conclusion

The FRS results have been examined for a regular and torsional irregular building in the current investigation. The primary goal of this research study is to highlight the influence of torsional irregularity with mass eccentricity on the Tri-directional FRS used in industrial buildings. It has been observed that the maximum peak spectral acceleration in the torsional irregular building is higher in both X–Y orthogonal directions as compared to the regular building. Furthermore, it is verified that the lateral design force for NSCs as per Indian standards is conservative than the lateral design force for NSCs as per FRS. There is no consideration of the building irregularity factor in the lateral design force formula for NSCs in the Indian standard.

The following are some key findings from the study.

1. Industrial buildings with variations in mass, stiffness, and strength result in further FRS intensification. Thus, for precise and protective non-structural component support design, the structural designer must use three-direction response spectra.
2. The IS 1893 (Part 4): 2015 – “Criteria for Earthquake Resistant Design of Industrial Structures” needs to expand on sections relevant to the FRS.
3. Using the moment of inertia factor for beam and column in the structural analysis could generate an equivalent response to that of the non-linear analysis.

It must be emphasized that the findings mentioned above and the conclusions are limited to low-rise reinforced concrete bare frame structures that were analysed and designed according to [36, 37, 40–42] for a given input. A broad parametric study is encouraged to generalise the results and investigate higher mode impacts on FRS in irregular buildings with and without infill walls.

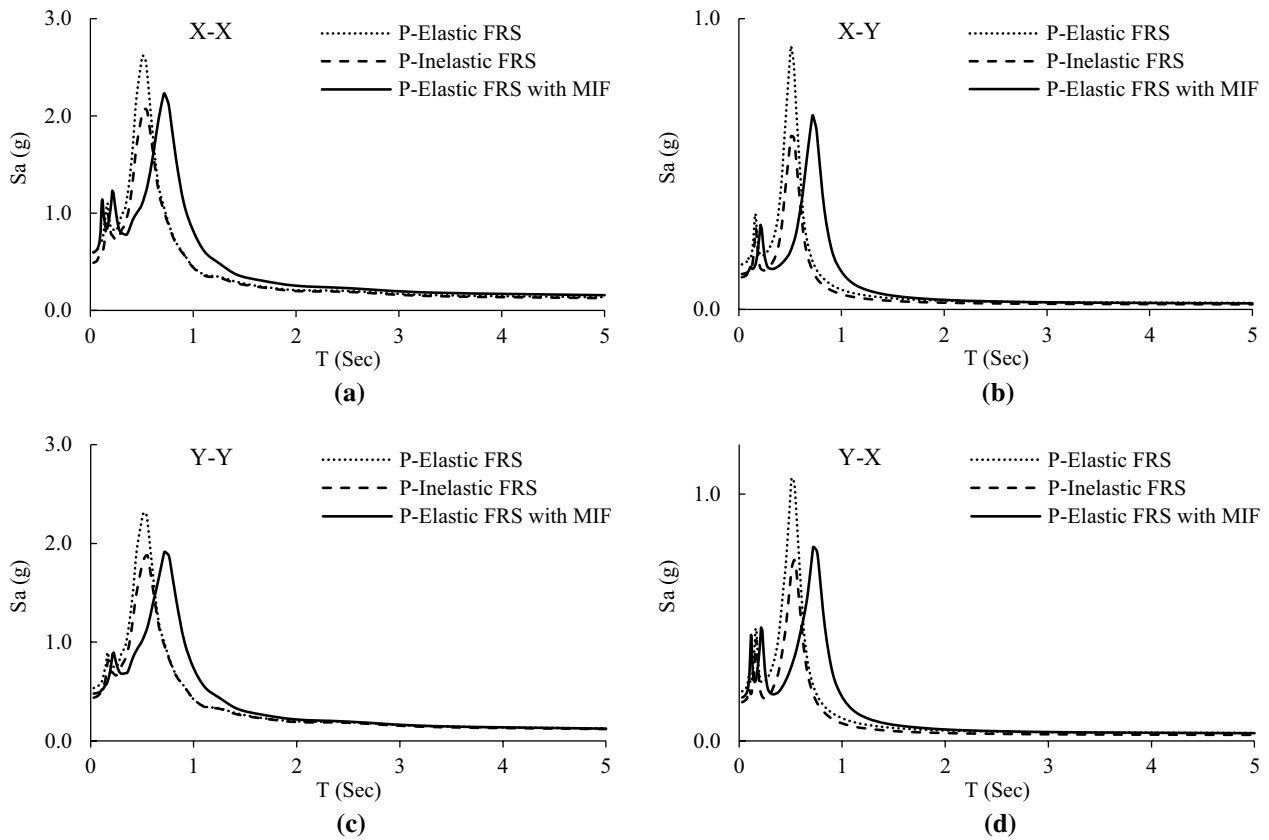


Fig. 9 FRS results at NSC location P

Table 8 NSC Design Forces at 3rd Floor

		As per FRS	As per IS 16700			
NSC Design Force Formula		$F_p = ma$	$F_p = z \left(1 + \frac{x}{h}\right) \frac{a_p}{R_p} I_p W_p$			
		where	where Z—Seismic Zone factor			
		m—mass of NSC	I _p —Importance factor of the NSC			
		a—peak spectral acceleration	R _p —component response modification factor			
			a _p —component amplification factor			
			W _p —weight of the NSC,			
			x—height of point of attachment of the NSE above top of the foundation of the building			
			h—overall height of the building			
			90			
		Input-Response direction				
		X-X	X-Y	Y-Y	Y-X	
NSC Design Forces (kN)	Elastic FRS	52	18	46	21	
	Inelastic FRS	41	12	38	15	
	Elastic FRS with MIF	45	13	38	16	

Funding No funding information available

Compliance with ethical standards

Conflict of interest On behalf of all authors, the corresponding author states that there is no conflict of interest.

References

- Perrone D, Calvi PM, Nascimbene R, Fischer EC, Magliulo G (2019) Seismic performance of non-structural elements during the 2016 Central Italy earthquake. *Bull Earthq Eng* 17(10):5655–5677. <https://doi.org/10.1007/s10518-018-0361-5>
- Biggs JM, Roesset JM (1970) Seismic analysis of equipment mounted on a massive structure. In: *Seismic design of nuclear power plants*, MIT press.
- USNRC Regulatory Guide 1.122 (1978) Development of floor design response spectra for seismic design of floor-supported equipment or components, Rev. 1
- Adam C (2001) Dynamics of elastic-plastic shear frames with secondary structures: shake table and numerical studies. *Earthquake Eng Struct Dynam* 30(2):257–277. [https://doi.org/10.1002/1096-9845\(200102\)30:2%3c257:AID-EQE7%3e3.0.CO;2-J](https://doi.org/10.1002/1096-9845(200102)30:2%3c257:AID-EQE7%3e3.0.CO;2-J)
- Agarwal AK, Datta TK (2003) Response of multiple-supported secondary system on torsionally coupled yielding primary system. *Advances in Vibration Engineering* 2(4):115–124
- Amin M, Hall WJ, Newmark NM, Kassawara RP (1971) Earthquake response of multiply connected light secondary systems by spectrum methods. In: *Proceedings of the 1st national conference on pressure vessels and piping*, New York 103–29.
- Bradley BA (2012) A ground motion selection algorithm based on the generalized condition intensity measure approach. *Soil Dyn Earthq Eng* 40:48–61. <https://doi.org/10.1016/j.soildyn.2012.04.007>
- Lucchini A, Franchin P, Mollaioli F (2017) Spectrum-to-spectrum methods for the generation of elastic floor acceleration spectra. *Procedia engineering* 199:3552–3557. <https://doi.org/10.1016/j.proeng.2017.09.514>
- Menon A, Magenes G (2011) Definition of seismic input for out-of-plane response of masonry walls: II. Formulation *Journal of Earthquake Engineering* 15(2):195–213. <https://doi.org/10.1080/13632460903456981>
- Singh AK, Ang AH (1974) Stochastic prediction of maximum seismic response of light secondary systems. *Nucl Eng Des* 29(2):218–230. [https://doi.org/10.1016/0029-5493\(74\)90124-1](https://doi.org/10.1016/0029-5493(74)90124-1)
- Singh MP (1980) Seismic design input for secondary systems. *J Struct Div* 106(2):505–517. <https://doi.org/10.1061/JSDEAG.0005371>
- Surana M, Singh Y, Lang DH (2018) Floor spectra of inelastic RC frame buildings considering ground motion characteristics. *J Earthquake Eng* 22(3):488–519. <https://doi.org/10.1080/13632469.2016.1244134>
- Villaverde R (2004) *Seismic analysis and design of non-structural components*. Earthquake engineering: from engineering seismology to performance-based engineering. CRC, Boca Raton, 1156–1220.
- Vukobratovic V, Fajfar P (2015) A method for the direct determination of approximate floor response spectra for SDOF inelastic structures. *Bull Earthq Eng* 13(5):1405–1424. <https://doi.org/10.1007/s10518-014-9667-0>
- Medina RA, Sankaranarayanan R, Kingston KM (2006) Floor response spectra for light components mounted on regular moment-resisting frame structures. *Eng Struct* 28(14):1927–1940. <https://doi.org/10.1016/j.engstruct.2006.03.022>
- Fragiadakis M, Vamvatsikos D, Papadrakakis M (2005) Evaluation of the influence of vertical stiffness irregularities on the seismic response of a 9-storey steel frame. In *Proceedings of the 4th European workshop on the seismic behavior of irregular and complex structures*, CD ROM. Thessaloniki.
- Singh MP, Moreschi LM, Suarez LE, Matheu EE (2006a) Seismic design forces I: Rigid non-structural components. *J Struct Eng* 132(10):1524–1532. [https://doi.org/10.1061/\(ASCE\)0733-9445\(2006\)132:10\(1524\)](https://doi.org/10.1061/(ASCE)0733-9445(2006)132:10(1524))
- Singh MP, Moreschi LM, Suarez LE, Matheu EE (2006b) Seismic design forces I: flexible non-structural components. *J Struct Eng* 132(10):1533–1543. [https://doi.org/10.1061/\(ASCE\)0733-9445\(2006\)132:10\(1533\)](https://doi.org/10.1061/(ASCE)0733-9445(2006)132:10(1533))
- ASCE/SEI 7-16 (2016) *Minimum Design Loads and Associated Criteria for Buildings and Other Structures*. American Society of Civil Engineers, Reston, Virginia.
- Duff C (1975) *Simplified Method for Development of Earthquake Ground and Floor Response Spectra for Nuclear Power Plant Design*. Technical Report. Atomic Energy of Canada Ltd., Sheridan Park, Ontario, Power Projects
- Singh M (1975) Generation of seismic floor spectra. *J Eng Mech Div* 101(5):593–607
- Biggs JM (1971) Seismic response spectra for equipment design in nuclear power plants, 1st SMIRT Conf., Berlin.
- Kapur KK, Shao LC (1973) Generation of seismic floor response spectra for equipment design. ASCE, In *Structural Design of Nuclear Plant Facilities*
- Chaudhuri SR, Villaverde R (2008) Effect of building non-linearity on seismic response of non-structural components: a parametric study. *J of Earthquake Eng* 134(4):661–670. [https://doi.org/10.1061/\(ASCE\)0733-9445\(2008\)134:4\(661\)](https://doi.org/10.1061/(ASCE)0733-9445(2008)134:4(661))
- Gupta AK (1990) *Response Spectrum Method in Seismic Analysis and Design of Structures*. Blackwell Scientific Publications, Boston, MA
- Phan LT, Taylor AW (1996) State of the art report on seismic design requirements for non-structural building components. Report NISTIR 5857, National Institute of Standards and Technology, Gaithersburg, MD.
- Politopoulos I (2010) Floor Spectra of MDOF nonlinear Structures. *J of Earthquake Eng* 14(5):726–742. <https://doi.org/10.1080/13632460903427826>
- Soong TT (1994) Seismic behavior of non-structural elements state-of-the-art report. In: *Proceedings, 10th European conference on earthquake engineering*.
- Yasui Y, Yoshihara J, Takeda T, Miyamoto A (1993) Direct generation method for floor response spectra. In: *Proceedings of the 12th International Conference on Structural Mechanics in Reactor Technology* 13 (4).
- An Y, Jiang Y, Ly B (2013) Direct generation of RRS from FRS. In: *Proceedings of the 22nd International Conference on Structural Mechanics in Reactor Technology*.
- Chen YQ, Soong TT (1988) Seismic response of secondary systems. *Eng Struct* 10(4):218–228. [https://doi.org/10.1016/0141-0296\(88\)90043-0](https://doi.org/10.1016/0141-0296(88)90043-0)
- Der Kiureghian A, Sackman J, Nour-Omid B (1983) Dynamic analysis of light equipment in structures: response to stochastic input. *J Eng Mech* 109(1):90–110. [https://doi.org/10.1061/\(ASCE\)0733-9399\(1983\)109:1\(73\)](https://doi.org/10.1061/(ASCE)0733-9399(1983)109:1(73))
- Igusa T, Der Kiureghian A (1985) Dynamic characterization of two-degree-of-freedom equipment-structure systems. *J Eng Mech* 111(1):1–19. [https://doi.org/10.1061/\(ASCE\)0733-9399\(1985\)111:1\(1\)](https://doi.org/10.1061/(ASCE)0733-9399(1985)111:1(1))
- Lai ML, Soong TT (1991) Seismic design considerations for secondary structural systems. *J Struct Eng* 117(2):459–472. [https://doi.org/10.1061/\(ASCE\)0733-9445\(1991\)117:2\(459\)](https://doi.org/10.1061/(ASCE)0733-9445(1991)117:2(459))
- Villaverde R (1997) Seismic design of secondary structures: state of the art. *J Struct Eng* 123(8):1011–1019. [https://doi.org/10.1061/\(ASCE\)0733-9445\(1997\)123:8\(1011\)](https://doi.org/10.1061/(ASCE)0733-9445(1997)123:8(1011))
- IS 1893-Part 4 (2015) *Criteria for earthquake resistant design of structures*. Industrial structures including stack like structures. Bureau of Indian Standards, New Delhi, India.

37. IS 1893-Part 1 (2016) Criteria for earthquake resistant design of structures. General provision and buildings. Bureau of Indian Standards, New Delhi, India.
38. Pacific Earthquake Engineering Research Center (2005) PEER Ground Motion <https://ngawest2.berkeley.edu/> Accessed 28 March 2020.
39. CSI, version 21 (2018) Integrated finite element analysis and design of structures basic analysis reference manual. Computers and Structures Inc, Berkeley (CA, USA).
40. IS 13920 (2016) Ductile Design and Detailing of Reinforced Concrete Structures Subjected to Seismic Forces –Code of Practice. Bureau of Indian Standards, New Delhi, India.
41. IS 16700 (2017) Criteria for structural safety of tall Concrete buildings –Code of Practice. Bureau of Indian Standards, New Delhi, India.
42. IS 456 (2000) Plain and Reinforced Concrete – Code of Practice (Fourth Revision). Bureau of Indian Standards, New Delhi, India.
43. IS 875-Part 1 (1987) Code of Practice for Design Loads (other than Earthquake) for Buildings and Structures: Part 1-Dead Loads (second revision). Bureau of Indian Standards, New Delhi, India.
44. IS 875-Part 2 (1987) Code of Practice for Design Loads (other than earthquake) for Buildings and Structures: Part 2- Imposed Loads (second revision). Bureau of Indian Standards, New Delhi, India.
45. Kumar R, Singh Y, Tripathi S (2011) Effect of building performance on floor response spectra. *J Struct Eng (Madras)* 37(6):422–426
46. Suarez LE, Singh MP (1987) Floor response spectra with structure–equipment interaction effects by a mode synthesis approach. *Earthquake Eng Struct Dynam* 15(2):141–158. <https://doi.org/10.1002/eqe.4290150202>
47. Araujo M, Macedo L, Marques M, Castro JM (2016) Code-based record selection methods for seismic performance assessment of buildings. *Earthq Eng Struct* 45(1):129–148. <https://doi.org/10.1002/eqe.2620>
48. Baker JW (2007) Measuring bias in structural response caused by ground motion scaling. 8th Pacific Conference on Earthquake Engineering, Singapore, Paper No. 56, CD ROM proceedings.
49. Cantagallo C, Camata G, Spacone E (2014) Seismic demand sensitivity of reinforced concrete structures to ground motion selection and modification methods. *Earthq Spectra* 30(4):1449–1465. <https://doi.org/10.1193/062812EQS226M>
50. Katsanos EI, Sextos AG, Manolis GD (2010) Selection of earthquake ground motion records: a state-of-the-art review from a structural engineering perspective. *Soil Dyn Earthq Eng* 30(4):157–169. <https://doi.org/10.1016/j.soildyn.2009.10.005>
51. Bradley BA (2013) A critical examination of seismic response uncertainty analysis in earthquake engineering. *Earthquake Eng Struct Dynam* 42(11):1717–1729. <https://doi.org/10.1002/eqe.2331>
52. Grant DN, Diaferia R (2013) Assessing adequacy of spectrum-matched ground motions for response history analysis. *Earthquake Eng Struct Dynam* 42(9):1265–1280. <https://doi.org/10.1002/eqe.2270>
53. Hancock J, Bommer JJ, Stafford PJ (2008) Numbers of scaled and matched accelerograms required for inelastic dynamic analyses. *Earthquake Eng Struct Dynam* 37(14):1585–1607. <https://doi.org/10.1002/eqe.827>
54. Senaldi I, Magenes G, Penna A, Galasco A, Rota M (2014) The effect of stiffened floor and roof diaphragms on the experimental seismic response of a full-scale unreinforced stone masonry building. *J Earthquake Eng* 18(3):407–443. <https://doi.org/10.1080/13632469.2013.876946>
55. Baker JW (2011) Conditional mean spectrum: tool for ground-motion selection. *J Struct Eng* 137(3):322–331. [https://doi.org/10.1061/\(ASCE\)ST.1943-541X.0000215](https://doi.org/10.1061/(ASCE)ST.1943-541X.0000215)
56. Bommer JJ, Acevedo AB (2004) The use of real earthquake accelerogram as input to dynamic analysis. *J Earthq Eng* 8(1):43–91. <https://doi.org/10.1080/13632460409350521>
57. Krawinkler H, Medina R, Alavi B (2003) Seismic drift and ductility demands and their dependence on ground motions. *Eng Struct* 25(5):637–653. [https://doi.org/10.1016/S0141-0296\(02\)00174-8](https://doi.org/10.1016/S0141-0296(02)00174-8)
58. Kumbhar OG, Kumar R (2020) Performance assessment of RC frame designed using force, displacement & energy-based approach. *Structural Engineering and Mechanics* 73(6): 699–714. <https://doi.org/10.12989/sem.2020.73.6.699>
59. Landge MV, Ingle RK (2020) Comparative study of floor response spectra for regular and irregular buildings subjected to earthquake. *Asian Journal of Civil Engineering* 22:49–58. <https://doi.org/10.1007/s42107-020-00297-1>
60. Shooshtari M, Saatcioglu M, Naumoski N, Foo S (2010) Floor response spectra for seismic design of operational and functional components of concrete buildings in Canada. *Can J Civ Eng* 37(12):1590–1599. <https://doi.org/10.1139/L10-094>
61. Rodríguez ME, Restrepo JI, Carr AJ (2002) Earthquake induced floor horizontal accelerations in buildings. *Earthquake Eng Struct Dynam* 31(3):693–718. <https://doi.org/10.1002/eqe.149>
62. Uma SR, Zhao JX, King AB (2010) Seismic actions on acceleration sensitive non-structural components in ductile frames. *Bull N Z Soc Earthq Eng* 43(2):110–125. <https://doi.org/10.5459/bnzsee.43.2.110-125>
63. Singh MP, Chang TS, and Suarez LE (1996) Floor response spectrum amplification due to yielding of supporting structure. In Proceedings of 11th World Conference on Earthquake Engineering.
64. Maddaloni G, Magliulo G, Cosenza E (2012) Effect of the seismic input on non-linear response of R/C building structures. *Adv Struct Eng* 15(10):1861–1877. <https://doi.org/10.1260/1369-4332.15.10.1861>
65. Petrone C, Magliulo G, Manfredi G (2015) Floor response spectra in RC frame structures designed according to Eurocode 8. Article in *Bulletin of Earthquake Engineering* 14(3):747–767. <https://doi.org/10.1007/s10518-015-9846-7>
66. Kanee ART, Kani IMZ, Noorzad A (2013) Elastic floor response spectra of non-linear frame structures subjected to forward-directivity pulses of near-fault records. *Earthquakes and Structures* Doi: <https://doi.org/10.12989/eas.2013.5.1.049>
67. Sankaranarayanan R, Medina RA (2007) Acceleration response modification factors for non-structural components attached to inelastic moment-resisting frame structures. *Earthquake Eng Struct Dynam* 36(14):2189–2210. <https://doi.org/10.1002/eqe.724>
68. ASCE/SEI 41-17 (2017) Seismic Evaluation and Retrofit of Existing Buildings. American Society of Civil Engineers, Reston, Virginia
69. Takeda T, Sozen MA, Nielsen NN (1970) Reinforced concrete response to simulated earthquakes. *J Struct Div* 96(12):2557–2573. <https://doi.org/10.1061/JSDEAG.0002765>
70. Flores FX, Garcia DL, Charney FA (2015) Assessment of floor accelerations in special steel moment frames. *J Constr Steel Res* 106:154–165. <https://doi.org/10.1016/j.jcsr.2014.12.006>
71. Wieser J, Pekcan G, Zoghi AE, Itani A, Maragakis M (2013) Floor accelerations in yielding special moment resisting frame structures. *Earthquake Spectra* 29(3):987–1002